Pion absorption on ^{3}He at $T_\pi = 62.5$ and 82.8 MeV

K. A. Aniol*
Department of Physics and Astronomy, California State University, Los Angeles, Los Angeles, California 90032 and Department of Physics, University of British Columbia, Vancouver, British Columbia, Canada V6T 2A6

A. Altman, R. R. Johnson, H. W. Roser,† R. Tacik,‡ and U. Wienands
Department of Physics, University of British Columbia, Vancouver, British Columbia, Canada V6T 2A6

D. Ashery, J. Alster, M. A. Moinester, and E. Piasetzky
Raymond and Beverly Sackler Faculty of Exact Sciences, Department of Physics, Tel-Aviv University, Ramat Aviv, Israel 69978

D. R. Gill and J. Vincent
TRIUMF, Vancouver, British Columbia, Canada V6T 2A3
(Received 21 October 1985)

Pion absorption in ^{3}He was studied at $T_\pi = 62.5$ and 82.8 MeV using nucleon-nucleon coincidences. For π^+ absorption on proton-neutron pairs the differential cross section is the same as that for $\pi^+ + d \rightarrow p + p$ except for an increase by a factor of about 1.5. For π^- absorption on the proton-proton pair, the differential cross section is asymmetric about 90°, indicating possible isospin mixing. The total cross sections $\sigma_{pn}(\pi^+)$ are 10.2±0.9 mb and 13.5±1.3 mb at 62.5 and 82.8 MeV and for $\sigma_{pp}(\pi^-)$ are 0.70±0.07 mb and 0.92±0.10 mb at 62.5 and 82.8 MeV. The three-body absorption cross sections for π^+ and π^- are found to be comparable to each other and show no strong energy dependence. The three-body absorption cross section $\sigma_3(\pi^+)$ is 6.7±2.5 mb and 5.7±2.3 mb and for π^-, $\sigma_3(\pi^-)$ is 8.7±1.4 mb and 6.5±2.0 mb at 62.5 and 82.8 MeV, respectively.

I. INTRODUCTION

Pion true absorption is a major fraction of the pion nucleus reaction cross section.[1,2] In the simplest description of pion absorption at least two nucleons are needed. Two-nucleon absorption in nuclei is frequently modeled after pion absorption in the deuteron. This clearly limits the nucleon pairs, for which a fundamental treatment of pion absorption can be attempted, to those with the deuteron quantum numbers ($T=0$, $S=1$, $L_{2N}=0$). However, nucleon pairs can couple to form other quantum numbers. As can be seen from Table I, pion absorption on the deuteron leads to states with isospin $T=1$ which allows formation of the Δ resonance as the intermediate state. In fact, this reaction is dominated by the $^1D_2$ final state, formed following an intermediate state with a Δ and nucleon in relative $L=0$. In order to study the complementary set of quantum numbers, pion absorption on a $^1S_0$ $T=1$ nucleon pair should be studied (Table I). The proton pair in the ground state of ^{3}He has, to a good approximation, these quantum numbers.

Recently, information on pion absorption on $T=1$, $S=0$ nucleon pairs has become available.[3–6] These studies have shown that the cross section for this reaction is a factor of 10–20 smaller than for pion absorption on the deuteron at bombarding energies from zero to 165 MeV. In addition, at 65 MeV (Ref. 5) the differential cross section for the process $\pi^- + pp \rightarrow p + n$ is asymmetric about 90° in the pion-2 nucleon center of mass, in contrast to the symmetric angular distribution for π^+ absorption. This asymmetry can be explained[3] by considering the possible intermediate state quantum numbers in the absorption process (Table I). Interference between odd and even partial waves can generate this asymmetry. For pion absorption on $T=1$, $S=0$, $L_{NN}=0$ nucleon pairs, an intermediate state of a delta resonance and a nucleon with $L_{\Delta N}=0$ cannot be formed thus suppressing absorption through Δ formation and generating sensitivity to non-Δ absorption mechanisms. Hence, it is of great interest to obtain the differential cross section for this reaction as a function of

TABLE I. Quantum numbers involved in pion absorption on nucleon pairs. The subscripts i, ΔN, and f refer to the initial nucleon pair, the ΔN intermediate system, and the final nucleon pairs. The orbital angular momentum of the π-2N system is denoted $l(\pi\text{-}2N)$.

$J_i\pi_i T_i$ $L_i=0$	$l(\pi\text{-}2N)$	$J^\pi_{\Delta N}, L_{\Delta N}$ $T_{\Delta N}=1$	J^π_f, L_f, T_f	$^{(2s+1)}L_f$
$1^+,0$	0	$1^-,1$	$1^-,1,1$	$^3P_1$
	1	$0^+,2$	$0^+,0,1$	$^1S_0$
		$2^+,0,2$	$2^+,2,1$	$^1D_2$
$0^+,1$	0	$0^-,1$	$0^-,1,1$	$^3P_0$
	1	no Δ	$1^+,0,0$	$^3S_1$
			$1^+,2,0$	$^3D_1$

pion bombarding energy. This will enable nondelta mechanisms of pion absorption to be studied.

The absorption on the $T=0$, $S=1$ pair in ^{3}He is also of interest, since it allows us to compare a well-known process (from the deuteron) in a different environment. What, for example, is the effect of the larger density in ^{3}He on the magnitude of the total two-nucleon absorption and the angular distribution? There is also an accumulating body of data which shows that pion absorption in nuclei may have significant multinucleon modes.[7] In large nuclei, the multinucleon absorption must be disentangled from final state interactions involving nucleons produced in the initial two-nucleon absorption event. Here, in ^{3}He, we have only one other nucleon and final state interactions are then as small as it is experimentally feasible to achieve. A detailed study of pion absorption on ^{3}He may allow investigation of genuine three-nucleon absorption mechanisms.

II. EXPERIMENTAL METHOD

A. Apparatus

In the present work we report studies of the ^{3}He(π^+2p)p and ^{3}He(π^-,pn)n reactions at 62.5 and 82.8 MeV. Two protons (for π^+) and proton-neutron (for π^-) were detected in coincidence. The protons were detected by NaI(Tl)-plastic scintillator telescopes and the coincident protons/neutrons were detected by an array of plastic scintillators.

A schematic drawing of our experimental setup is shown in Fig. 1. This is very similar to the arrangement used in Ref. 5 except for the ^{3}He target. Counters $S3$, $S5$, and $S6$ (Nuclear Enterprises NE110) were used as vetoes. A beam event required a coincidence of $S1$ and $S2$ and no $S3$. Counter $S1$ was 7.6 cm in diameter and $S2$ was (2.5×3.8) cm^2. The pion beam was monitored by S_1S_2 and independently by the coincidence of $\mu_1\mu_2$ which registered pion decay in flight. In the coincidence mode we require a coincidence between the beam counters, one of the

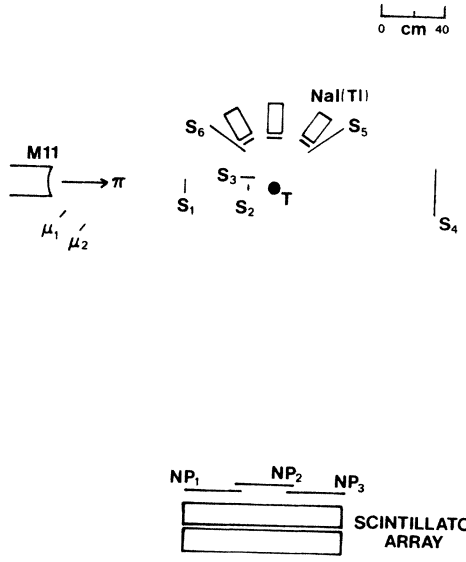

FIG. 1. Experimental arrangement. The target is at T.

NaI telescopes and the large array of plastic scintillators (Nuclear Enterprises NE110). Typically, one of the NaI telescopes was set at an angle (the conjugate angle) corresponding to the kinematics of the proton pair from $\pi^+ + d \rightarrow p + p$ with respect to the scintillator array. Thus, we also measured simultaneously for each conjugate angle two nonconjugate angles in the remaining telescopes.

The scintillator array, which was used both for pp and pn coincidences, was formed from two layers, each layer consisting of seven bars stacked horizontally. The bars were (15×15×105) cm^3, positioned at 2.2 m from the target and were viewed from each end by a photomultiplier tube. The relative timing between the ends of a bar determined the horizontal location of a hit (to within 3 cm). The time-of-flight between the beam counters and the bars gave the energy of the particle. In this way we determined the vertical and horizontal spatial distribution and the energy distribution of nucleons in coincidence with the NaI telescopes. The neutron detection efficiency of the bars was calculated for a threshold of 1 MeV set with a ^{60}Co source.[8] The uncertainty in the neutron detection efficiency is 12%. In front of this array, three thin scintillators $NP1$, $NP2$, and $NP3$ distinguished neutrons from protons. As well, the overlaps of $NP1$ with $NP2$ and of $NP3$ with $NP2$ were used for position calibration and position resolution determination.

The NaI telescopes consisted of plastic scintillator (Nuclear Enterprises) ΔE counters of dimension (6.8×7.8×0.64) cm^3 followed by NaI counters (10×10×20) cm^3. This arrangement allowed us to identify the particle species incident on the telescopes. The telescopes were separated from each other by 30° and subtended a solid angle of 42.5 msr for the two backward telescopes and 46.0 msr for the forward telescope.

A new ^{3}He target was constructed for this measurement (Fig. 2). Very little extraneous mass was in the beam with this target. Its 7.25 cm diameter cylindrical design enabled unimpeded observation by all three NaI telescopes and the array simultaneously.

B. Absolute normalization

The beam composition at TRIUMF is readily measured event by event utilizing the time-of-flight of beam particles through the channel. The π^+ fraction of the beam was 83% and 90% at 65 and 85 MeV, respectively, and for π^- it was 64% and 74%. In some cases the π^+ rate was as high as 2.7×10^6 per second. The beam profile at the target was measured. Our beam counters intercepted 77% of the beam from the $M11$ channel.

The solid angles were known both from the geometry of our setup and from measurement of the $\pi^+ + d \rightarrow p + p$ reaction. The cross sections we measured for this reaction at 65 MeV agreed with the published values of Ref. 9 to within 4% or better.

The density of the ^{3}He target was determined in three ways. First we made a range measurement of 41.68 MeV μ^+ passing through the target compared to a dummy target made of the same material except without the ^{3}He. This gave a density of ^{3}He nuclei of (1.49±0.08)

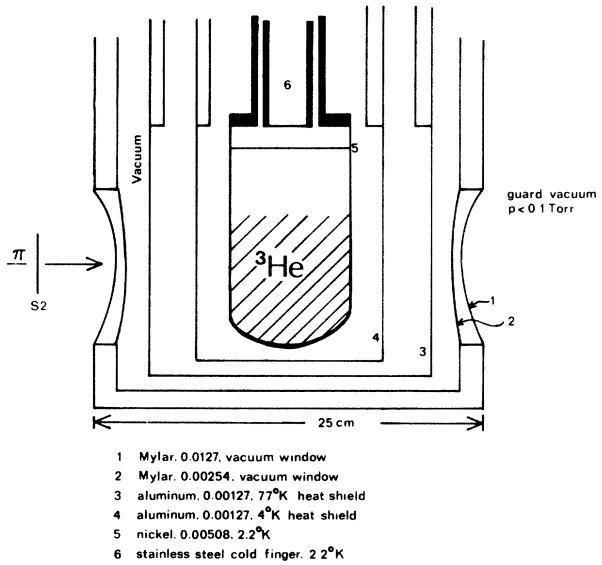

FIG. 2. Cryogenic ^{3}He target.

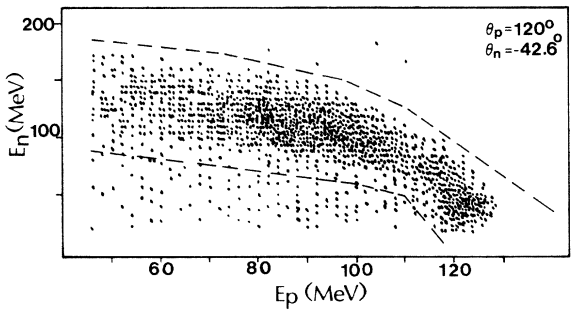

FIG. 3. Scatterplot of proton energy versus neutron energy for $\theta_p = 120°$, $\theta_n = -42.6°$, and $T_\pi = 82.8$ MeV. The dashed lines are the cuts imposed when projecting the proton energy spectrum. This scatterplot is from π^- absorption.

$\times 10^{22}/\text{cm}^3$. Second, we measured the elastic scattering of 65 MeV π^+ from the target at five angles between 60° and 120° and compared it to the elastic scattering data of Ref. 10. This gave us a density of $(1.43\pm0.06)\times10^{22}/\text{cm}^3$. Third, we measured the coincidences from the reaction $\pi^- + {}^3\text{He} \rightarrow \text{n} + \text{d}$ at 35° for 65 MeV and at 35°, 50°, and 65° for 85 MeV bombarding energies and used the data from the time reversed isospin symmetric reaction $\text{p} + \text{d} \rightarrow \text{t} + \pi^+$ from Ref. 11. The target density from this procedure was $(1.15\pm0.18)\times10^{22}/\text{cm}^3$. This third technique was the one that was used in Ref. 5. There is evidence, to be discussed in the next subsection, that the $\text{p} + \text{d} \leftrightarrow \text{t} + \pi^+$ and $\text{n} + \text{d} \leftrightarrow \pi^- + {}^3\text{He}$ reactions are not exactly related by isospin Clebsch-Gordan coefficients. For this reason we use the target thickness as determined from the range measurement. This value and the one determined by elastic scattering agree with the value deduced from the target temperature and geometry.

Background in the coincidence yields was minimized by imposing three-body kinematics conditions on the coincident nucleon's energies. In Fig. 3 we show a plot for the full target of neutron energy in the scintillator array ($\theta_n = 42.6°$) versus the coincident proton energy ($\theta_p = 120°$) in the NaI telescope. The dashed lines indicate the portion of the plot accepted in the analysis. It is seen that the three-body kinematic locus is enhanced compared to the region between the energy axes and the inner dashed line. This region is populated by reactions involving nuclei more massive than ^{3}He. The background for the π^- runs at the nonconjugate angles was typically 11% of the full target yield and at the conjugate angle it was typically 5%. For π^+ runs it was negligible.

Accidental coincidences were infrequent and could be measured by counting the number of events where the neutron energy was above the upper dashed line (i.e., in a nonphysical region). The accidental rate was less than 4% of the true coincidence rate for the full target. Most of the accidental coincidences were due to the high count rate suffered by the scintillator array when it was at the most forward angles.

C. Corrections

Corrections were made for reaction losses suffered by deuterons, protons, and pions in the NaI detector. In the case of monoenergetic deuteron and pion detection, the correction was simply a multiplicative factor determined in an energy dependent fashion. For protons we developed an unfolding procedure because protons of interest are spread over many MeV. These corrections were done using reaction loss measurements and amounted to typically 10%[12]. In addition, for pions, decay in flight from the target to the detectors was included, and the decay of the μ^+ (from the decay of the stopped μ^+ in the NaI counter) was accounted for by excluding the high energy tail on the elastic π^+ peak. This latter correction depends on the gate width used in integrating the NaI pulse, in our case 300 ns, and was about 13%. The π^+ 65 MeV elastic scattering data[10] were numerically averaged over the finite detector and target sizes in determining the target density. The $M11$ channel was set for 65 and 85 MeV which corresponds to energies in the center of our target of 62.5 and 82.8 MeV.

III. RESULTS

A. Determination of the nucleon-nucleon angular correlation

In the following discussion we will be referring to "two-body" (2N) and "three-body" (3N) absorption processes. In the former we look at events where the pion energy is shared between two nucleons only, the third nucleon acting as a spectator and carrying only the momentum it had as internal momentum in the ^{3}He nucleus prior to the absorption process. These events are concentrated in a part of the energy spectrum when the two nucleons are detected at the conjugate angles. The 3N absorption contains events where all three nucleons acquired a significant amount of energy from the absorption process. These events can be distributed all over phase space and

therefore exist in both conjugate and nonconjugate geometries.

Because of the finite momentum of the nucleon pair in the ^{3}He nucleus, the angular correlation of the proton-proton or proton-neutron coincidence has a finite width. The angular acceptance of the scintillators array is finite and we must make an estimate of the fraction of two-nucleon absorptions that does not get recorded because one of the nucleons falls outside of the solid angle of the scintillator array. In addition nucleon-nucleon coincidences are not solely from two-body absorption (2N), but will include some fraction of three-body absorption events (3N). The three-body absorption at the conjugate angles (where the 2N absorption peaks) can be estimated by looking at the coincidences in the nonconjugate telescopes. This is done by assuming that the matrix element of the three-body absorption is independent of the energy of the outgoing nucleons and their angles. The distribution of the 3N absorption is then determined by three-nucleon phase space, normalized to the experimentally determined magnitude obtained at the nonconjugate angles. Our measurements show that the magnitude of the 3N absorption is not strictly given by the three-nucleon phase space distribution. The shape of the proton energy spectrum is consistent with that expected from the phase space factor (Fig. 4) but there is a variation of the magnitude with angles of the coincident pair. In Table II we list the values of the phase space factors for various pairs of angles of the nucleon pairs. There is an rms variation of about 30% from the mean value for these factors.

In the analysis, the scintillator array is divided into a matrix of 7×7 cells, for each of which a spectrum like that of Fig. 3 is obtained. We subtract a 3N absorption

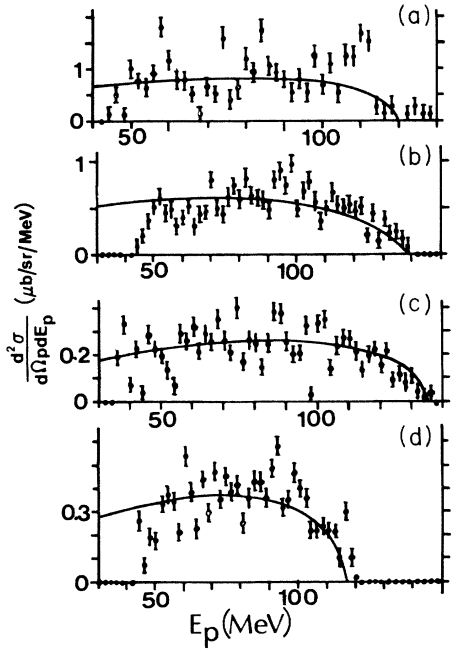

FIG. 4. Proton energy distributions for off conjugate coincidences. The solid angle of the scintillator array in (a) and (b) was 0.189 sr and in (c) and (d) it was 0.220 sr. The spectra are (a) 65 MeV π^+ (80°, −114°), (b) 85 MeV π^+ (40°, −59.2°), (c) 85 MeV π^- (70°, −59.2°), (d) 65 MeV π^- (90°, −45°), where the angles (θ_p, θ_{array}) refer to the angle of the NaI telescope for the protons and the angle of the array in which the coincident nucleon was detected, respectively. The solid lines are the spectral shapes expected from a purely phase space distribution.

TABLE II. Estimates of the 3N absorption cross sections. Phase space factors are determined from the nonconjugate angle coincidences. The first column for each energy lists the angles of the NaI, θ_p, and the scintillator array, θ_N. The second and third columns are the phase space factors f defined as,

$$\frac{d^3\sigma(3N)}{d\Omega_p d\Omega_N dE_p} = \frac{f p_p p_N^2}{8 E_N E_3} \frac{\mu b}{sr^2\,MeV},$$

where p_p, p_N, E_p, and E_N are the momenta and energies of the detected particles p,N and E_3 is the energy of the remaining nucleon. All momenta and energies are expressed in units of MeV/c and MeV.

	62.5 MeV			82.8 MeV	
(θ_p,θ_N)	$f(\pi^+)$	$f(\pi^-)$	(θ_p,θ_N)	$f(\pi^+)$	$f(\pi^-)$
(65, −133)	0.50±0.09	0.15±0.03	(65, −129.9)	0.37±0.03	0.11±0.02
			(95, −129.9)	0.18±0.06	0.06±0.01
(80, −114)	0.52±0.05		(80, −110.8)	0.45±0.09	0.11±0.02
			(110, −110.8)	0.20±0.04	
(35, −97)	0.19±0.02		(35, −93.5)	0.16±0.02	
(95, −97)	0.36±0.04		(95, −93.5)		0.10±0.02
(110, −114)	0.26±0.05		(50, −77.8)	0.19±0.02	0.05±0.01
(110, −81)		0.14±0.03	(110, −77.8)		0.10±0.02
(40, −62)	0.36±0.07		(40, −59.2)	0.29±0.05	0.08±0.02
			(70, −59.2)		0.09±0.02
(60, −45)		0.15±0.03	(60, −42.6)	0.28±0.09	0.08±0.02
(90, −45)		0.19±0.04	(90, −42.6)		0.18±0.04
$\langle f_{65}\rangle$	0.37±0.13	0.16±0.02	$\langle f_{85}\rangle$	0.26±0.10	0.10±0.03

TABLE III. Laboratory differential cross sections for the 2N absorption mechanisms of $\pi^{\pm}$ on ^{3}He.

			π^+				π^-			
θ_L[a] (deg)	Fraction[b]	Energy limits[c] (MeV)	$\frac{d\sigma^M}{d\Omega}$(2N + 3N)[d] ($\mu$b/sr)	$\frac{d\sigma}{d\Omega}$(3N)[e] (μb/sr)	$\frac{d\sigma}{d\Omega}$(2N)[f] (μb/sr)	Energy limits (MeV)	$\frac{d\sigma}{d\Omega}^M$(2N + 3N) ($\mu$b/sr)	$\frac{d\sigma}{d\Omega}$(3N)[g] (μb/sr)	$\frac{d\sigma}{d\Omega}$(2N) (μb/sr)	$\frac{d\sigma}{d\Omega}$(2N)[h] (μb/sr)
				62.5 MeV						
35	0.79±0.06	76–150	2281±23	54±10	2818±217	90–148	72.7±1.5	16.8±2.1	70.8±6.3	65.5±11.8
50	0.78±0.08	54–142	1526±20	69±24	1868±196					31.4±10.1
65	0.85±0.10	40–136	951±15	76±27	1029±126					16.9± 7.5
80	0.89±0.10	44–132	708±11	71±25	716± 86	78–128	26.2±1.0	16.5±2.1	11.4±2.9	11.3± 6.0
100	0.87±0.09	46–124	946±22	63±22	1015±109					
110										49.3±10.1
120	0.90±0.05	40–120	1437±14	63±22	1527± 90	40–114	117.5±3.5	44 ±6	81.7±9.0	75.5±12.3
				82.8 MeV						
35	0.75±0.05	70–160	2807±22	55±21	3669±249	88–156	85.9±2.1	15.9±4.8	93.3±9.4	
50	0.80±0.04	70–160	1954±15	55±21	2373±123	84–148	49.7±1.3	15.4±4.6	42.9±6.3	
65	0.83±0.05	60–160	1233± 9	59±23	1414±90	74–138	29.1±0.9	16.2±4.9	15.5±6.1	
80	0.87±0.04	56–150	953± 5	59±23	1027±54	78–140	25.2±0.9	15.5±4.7	11.1±5.5	
100	0.88±0.04	40–140	1271± 9	62±24	1374±69	64–130	61.3±1.8	17.1±5.1	50.2±6.6	
120	0.90±0.04	40–130	1925±13	57±22	2075±96	40–122	133.4±3.0	36 ±11	108.2±13.6	

[a]Laboratory angle of proton detected in a NaI telescope.

[b]Calculated accepted fraction of coincidences from the double Gaussian fit of the proton-proton angular correlation.

[c]Energy limits in MeV of the integration of the proton spectrum.

[d]Total measured cross section in μb/sr for coincidences between the NaI telescope and the scintillator array (SA) ($\Delta\Omega_{SA}=0.220$ sr).

[e]Computed 3N absorption contribution to $(d\sigma^M/d\Omega)(2N + 3N)$. This contribution is integrated over the energy bin in the third column and over the angular acceptance of the scintillator array using the averaged values of f in Table II.

[f]Deduced laboratory differential cross section for proton emission into the angle θ_L for 2N absorption. This quantity is

$$\frac{d\sigma(2N)}{d\Omega} \equiv \left| \frac{d\sigma}{d\Omega}^M (2N+3N) - \frac{d\sigma}{d\Omega}(3N) \right| / \text{fraction} .$$

[g]Same as footnote e above, except at 120° at both energies the average f factor is clearly too small. At this angle we chose f to fit the energy spectrum in the low energy portion of the spectrum away from the two-body peak.

[h]These are the π^- results from Ref. 5 normalized by a factor of 0.83 as described in the text.

contribution computed for each cell from the phase space distribution and obtain the 2N distribution over the 49 cells. This 2N distribution is then integrated over the measured nucleon energies and fitted by a double Gaussian in horizontal and vertical angles. From the parameters of the double Gaussian we can estimate the fraction of the 2N coincidences that the scintillator array accepts. The accepted fraction, which is angle dependent, varies between (0.79±0.05) and (0.90±0.05).

The angular correlation is readily measured with $\pi^+ + {}^3\text{He} \rightarrow \text{pp} + \text{p}$ because the yield is large. The two-nucleon absorption is also very much larger (see Table III) than the part of the 3N absorption under the 2N peak so that the subtraction of the 3N contribution from the coincidence yield introduces little uncertainty (at the conjugate angle) in the angular correlation. The full width at half maximum of the angular correlation, after subtraction of the finite geometrical effects (in quadrature), is angle dependent and varies in the range 12.4°±1.0° for the proton-proton coincidences.

In the case of $\pi^- + {}^3\text{He} \rightarrow \text{pn} + \text{p}$, the two-nucleon absorption is of comparable magnitude to the background contribution from three-nucleon absorption. In principle the 2N and 3N absorption amplitudes add coherently, whereas in our subtraction technique we have assumed they add incoherently. Experimentally there is no way to separate events arising from the 2N absorption and 3N absorption at the conjugate angles within the 2N peak. The fact that the angular distribution of the phase space factors (Table II) does not show correlation with the (2N) angular distribution gives support to the incoherence assumption. We found that the angular correlation of the p-n pair from the 2N absorption of π^- is consistent with that measured from the p-p angular correlation of 2N π^+ absorption. We, therefore, used the accepted fractions deduced from the p-p angular correlation for that of the p-n angular correlation.

B. Differential cross sections for pion absorption on nucleon pairs

In Figs. 5–7 we show energy spectra taken at conjugate geometries. After subtracting the 3N background and correcting for the accepted fraction of the angular correlation discussed in the previous subsection, a differential cross section for the 2N absorption is obtained. In Fig. 8 we display the differential cross sections for $\pi^\pm$ absorption on nucleon pairs (T=0, S=1 and T=1, S=0) at T_π=62.5 MeV. Included in Fig. 8 are the data from Ref. 5, renormalized by a factor of 0.83. This renormalization is necessary because the method of determining the target thickness in Ref. 5 relied upon monitoring the $\pi^- + {}^3\text{He} \rightarrow \text{d} + \text{n}$ reaction and assuming that this monitor reaction can be given exactly by the time reversed isospin symmetric reaction $\text{p} + \text{d} \rightarrow \text{t} + \pi^+$ (see Sec. II B). The ratio of cross section for $(\pi^- + {}^3\text{He} \rightarrow \text{pn} + \text{n})/(\pi^- + {}^3\text{He} \rightarrow \text{d} + \text{n})$ in the present measurement remains the same as in Ref. 5, but the differential cross section for the $\pi^- + {}^3\text{He} \rightarrow \text{d} + \text{n}$ process has now been measured rather than deduced from the $\text{p} + \text{d} \rightarrow \text{t} + \pi^+$ reaction. This measurement showed (see the next subsection) that the cross section for $\pi^- + {}^3\text{He} \rightarrow \text{d} + \text{n}$ is different from

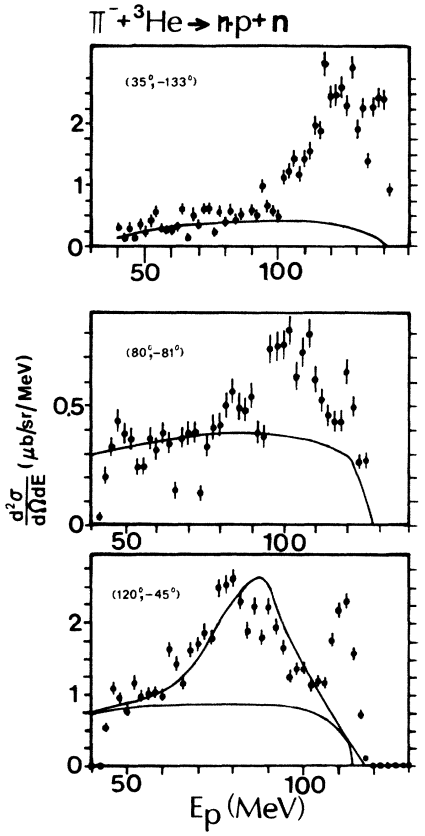

FIG. 5. Proton energy spectra for 62.5 MeV π^- absorption on ^{3}He at the conjugate angles (θ_p,θ_n) indicated in the figure. The lines drawn in are the expected three-body contributions deduced from the off conjugate spectra (such as in Fig. 4, for example). In addition, at (120°, −45°) the shape of the spectrum from the π^+-induced reaction for the same pair of angles is superimposed.

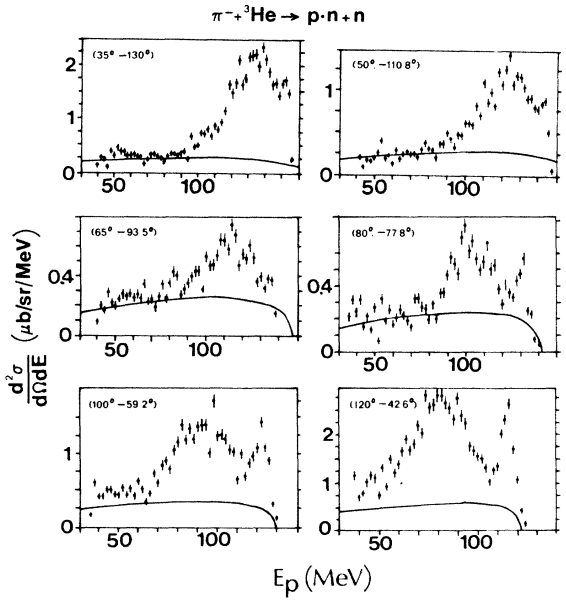

FIG. 6. This is the same as in Fig. 5 except for T_{π^-}=82.8 MeV.

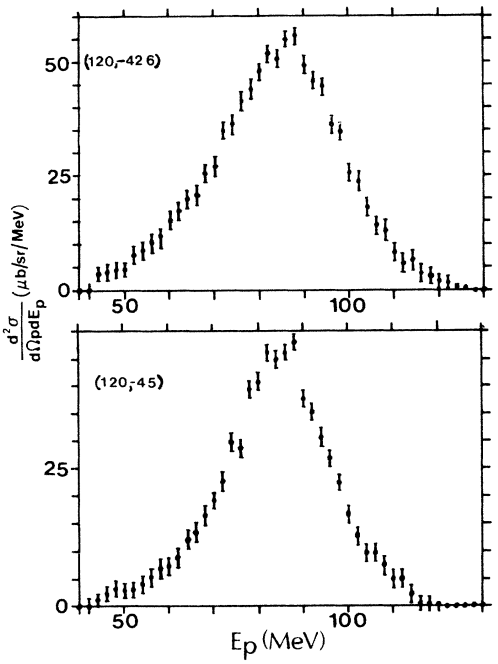

FIG. 7. Proton energy spectra from π^+ absorption on ^{3}He. Two conjugate angles are displayed. Top, 82.8 MeV; bottom, 62.5 MeV.

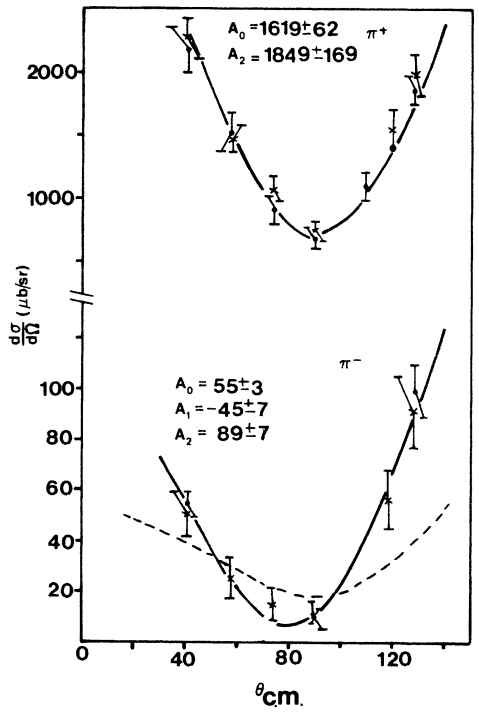

FIG. 8. Angular distribution for two-nucleon absorption of $\pi^\pm$ on ^{3}He at 62.5 MeV. The coefficients A_i are the Legendre polynomial coefficients expressed in μb/sr. The angular distributions are plotted in the π-d center-of-mass system. The dashed line is from Ref. 23.

that deduced from $p + d \rightarrow t + \pi^+$ data[11] that are available in our energy region.

The differential cross sections in Figs. 8 and 9 are displayed in the π^-d center-of-mass system. This reference frame is suggested by the low momentum of the recoiling spectator nucleon as can be deduced from the narrowness of the peaks in Fig. 5 and 6 or equivalently from the narrowness of the angular correlation. The curves in Figs. 8 and 9 are Legendre polynomial fits and the coefficients were corrected for the finite size of the target and detector solid angle. This correction was less than one percent for the A_2 coefficient and about one percent for the A_0 coefficient. For the case of π^- absorption on the ($T=1$, $S=0$) nucleon pair there is a significant asymmetry about 90°. In the case of π^+ absorption on the ($T=S$, $S=1$) nucleon pair the angular distribution is symmetric. In Table III we list the laboratory differential cross sections for $\pi^\pm$ absorption on nucleon pairs at our two bombarding energies.

In the case of π^- absorption on the ($T=1$, $S=0$) pairs, we also observe a peak at the end of the proton energy spectrum (Figs. 5 and 6). This final state interaction peak corresponds to a proton recoiling against two neutrons which have comparable vector momenta. The lines in the figures are the expected 3N phase space contribution extrapolated from the nonconjugate angles and, in the case of Fig. 5 (120°, −45°), the shape of the proton spectrum from the $\pi^+ + {}^3\text{He} \rightarrow pp + p$ reaction at the same pair of angles.

C. The two-body breakup: $\pi^- + {}^3\text{He} \rightarrow n + d$

The measurement of the $\pi^- + {}^3\text{He} \rightarrow n + d$ differential cross section was done in two stages. In the first part, the

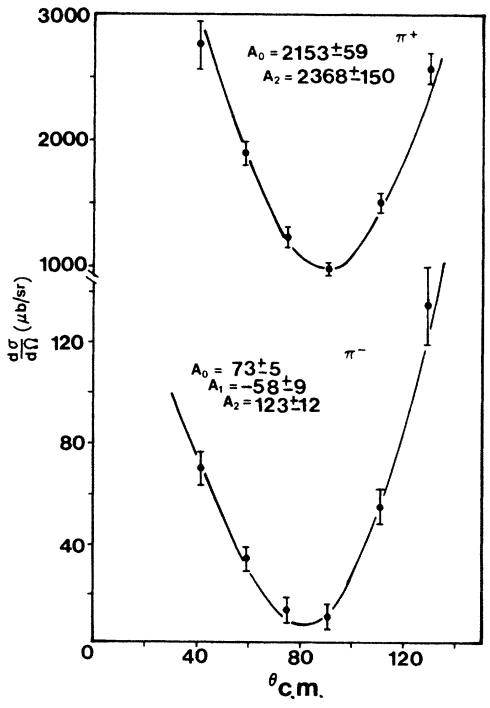

FIG. 9. This is the same as Fig. 8 except $T_\pi = 82.8$ MeV.

shape of the angular distribution was measured with the target described in Ref. 5. In the second part, the measurement of the differential cross section was limited to deuteron angles forward of 65° in the laboratory with the thicker target (Fig. 2). In Fig. 10 we compare our results with those from the $p + d \rightarrow t + \pi^+$. There appears to be a difference in the shape of the two angular distributions with the $^3He + \pi^- \rightarrow n + d$ reaction having a smaller cross section for $\theta \geq 110°$ (up to 17%) and a bigger cross section for $\theta_n \leq 110°$ than the $p + d \rightarrow t + \pi^+$ reaction. The ratio $\sigma(n + d \rightarrow \pi^- + {}^3He)/\sigma(n + d \rightarrow \pi^0 + t)$ (Ref. 13) also deviates from unity. In our case the differences between $^3He + \pi^- \rightarrow n + d$ and $p + d \rightarrow t + \pi^+$ may be due to absolute normalization errors in these two separate experiments. The error bars on our $^3He + \pi^-$ data are relative only. There is an overall normalization error of 15% from the target thickness uncertainty and the neutron detection efficiency calculation.

We observe that the differential cross sections at 62.5 and 82.8 MeV pion bombarding energy are equal within experimental error. This behavior is in accord with that seen in $p + d \rightarrow t + \pi^+$.[11,13] However, the cross sections at 50 and 100 MeV (Ref. 14) are systematically smaller than our results by a factor of about 2. Such a marked oscillatory behavior in the magnitude of $d\sigma/d\Omega$ over this energy interval would be surprising. Calculations[15] show a monotonic behavior of the differential cross section with energy. Another piece of the reaction cross section related to this two-body breakup is the "final-state-interaction" peak. Rather than the n-d final state, we now have the p-(2n) final state. Being barely separable from the (2N) peak, it is hard to derive precise results on this reaction. It is possible to determine that it is forward peaked in the c.m. systems and has a magnitude of about 50 μb (at 65 MeV bombarding energy).

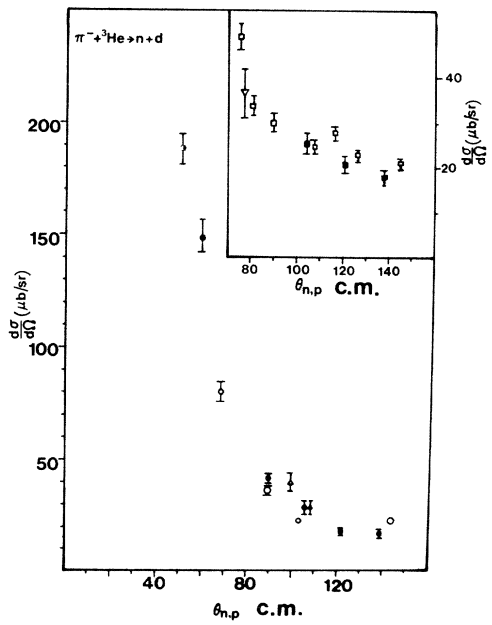

FIG. 10. Differential cross section of the $\pi^- + {}^3He \rightarrow n + d$ reaction measured in this experiment compared to the $\pi^+ + t \rightarrow p + d$ measurements. The symbols are ●, 62.5 MeV, ■, 82.8 this experiment; ○, T_{π^-}(equivalent) = 66.1 MeV; □, T_{π^-}(equivalent) = 82.7 MeV from $p + d \rightarrow t + \pi^+$ (Ref. 11); △, T_{π^-}(equivalent) = 67.5 MeV from $p + d \rightarrow \pi^o + {}^3He$ (Ref. 16).

D. The total two- and three-nucleon absorption cross sections

We describe the three-nucleon absorption cross section (see Table II) by the factor f in the expression

$$\frac{d^3\sigma}{d\Omega_p d\Omega_N dE_p} \equiv \frac{f p_p p_N^2}{8 E_N E_3}, \tag{1}$$

where p,N are the detected particles and particle 3 is undetected. We can cast our expression into that normally associated with an element of three-body differential phase space[17] as follows:

$$d\sigma = f \frac{\delta(M - E_p - E_N - E_3)}{2E_3} \frac{d^3p_p}{2E_p} \frac{d^3p_N}{2E_N}. \tag{2}$$

Finally, letting P be the total four-momentum, the integral over three-body phase space can be evaluated as

$$R_3(|P|, M_p, M_N, M_3) = \int_0^{p_3^{max}} \frac{d^3p_3}{2E_3} R_2(|P - P_3'|, M_p, M_N), \tag{3}$$

where the two-body phase space R_2 is

$$R_2(|Q|, M_1, M_2) = \frac{\pi[Q^4 - 2Q^2(M_1^2 + M_2^2) + (M_2^2 - M_1^2)^2]^{1/2}}{2Q^2}. \tag{4}$$

In these expressions P, P_3', and Q are four-momenta and p_p, p_N, and p_3 are the three-momenta. The energies E_i are given by $E_i^2 = p_i^2 + M_i^2$. Thus, R_2 and R_3 are the invariant phase space. In the case of π^+ absorption on ^{3}He, there are three protons in the final state, any of which could be labeled by p, N, or 3. There are, therefore, 3! ways of detecting a three-body absorption event with π^+. For π^- absorption we have two neutrons and one proton and thus 2! ways of detecting a three-body absorption with π^-. The total three-body absorption cross sections are then

$$\sigma_{3N\pi^+} = \frac{f_+}{3!} R_3(\pi^+ + {}^3He \rightarrow p + p + p), \tag{5a}$$

$$\sigma_{3N\pi^-} = \frac{f_-}{2!} R_3(\pi^- + {}^3He \rightarrow p + n + n). \tag{5b}$$

The results are shown in Table IV.

In addition to the nucleon-nucleon coincidence measurements at the nonconjugate angles we can extract the π^+ three-nucleon absorption cross section σ_{3N} from singles measurements once the two-nucleon absorption cross section σ_{2N} is known. This is possible at 62.5 MeV because no knockout protons are expected to be detected.

TABLE IV. Total absorption cross sections for two- and three-nucleon events.

	π^+			π^-	
T_π	a	b	c	a	b
(MeV)	σ_{2N}	σ_{3N}	σ_{3N}	σ_{2N}	σ_{3N}
62.5	10.2±0.4	6.7±2.4	3.6±0.4	0.70±0.04	8.7±1.1
82.8	13.4±0.4	5.7±2.2		0.92±0.06	6.5±1.9

[a] σ_{2N} in mb from coincidence data—errors are relative. There is an overall normalization error of 9% for π^+ and 15% for π^-.
[b] σ_{3N} in mb from coincidence nonconjugate data.
[c] σ_{3N} in mb from singles. For phase space normalized to data between 50° and 120° $\sigma_{3N}=3.1\pm0.5$ mb.

At each angle the differential cross section can be expressed as,

$$\frac{d\sigma_{3N}(\theta)}{d\Omega}=R\left[\frac{d\sigma_{tot}(\theta)}{d\Omega}-\frac{d\sigma_{2N}(\theta)}{d\Omega}\right]. \quad (6)$$

Here $d\sigma_{tot}(\theta)/d\Omega$ is the total singles differential cross section measured within certain proton energy limits. The factor R accounts for the portion of the proton energy spectrum (assumed to be given by the phase space) which is not within the integration limits.

In Fig. 11 we present $d\sigma_{3N}(\theta)/d\Omega$ as described above. The curve in Fig. 11 is the expected differential cross section (normalized to the points between 50° and 120°) if the only dependence were on phase space. It is seen that the angular dependence is similar to that expected from phase space except that there is too large a change between 50° and 35°. This forward peaking is reminiscent of the $^3\mathrm{He}+\pi^-\rightarrow\mathrm{n}+\mathrm{d}$ reaction, but there is no evidence in the singles spectra of a final state interaction peak which is the analog of the n + d final state.

As in the case of the coincidence spectra we can define phase space factors f_s for the singles spectra by

$$\frac{d\sigma_{3N}(\theta)}{d\Omega}=f_s R_3(\theta). \quad (7)$$

$R_3(\theta)$ is calculated in the laboratory frame from Eqs. (3) and (4). Note that in this case we neglect the angular integration in Eq. (3). The factor f_s is taken from the $50°\leq\theta\leq120°$ range since the 35° point deviates significantly from phase space.

$$f_s=(8.5\pm1.5)\times10^{-2}\ \mu\mathrm{b/sr}. \quad (8)$$

Then the total cross section σ_{3N} is

$$\sigma_{3N}=\frac{f_s}{3}\int d\Omega R_3(\theta). \quad (9)$$

We divide by three because there are three ways of detecting the 3N absorption event (i.e., three protons).

As an alternative way of integrating $d\sigma_{3N}/d\Omega$, the data (including the 35° point) were fitted with Legendre polynominals ($l=0,1,2$). This cross section is 3.6±0.4 μb and agrees with the one obtained using phase space integration. In Table IV we list the total cross sections for three-nucleon and two-nucleon absorption as determined from the above equations and the f factors from Table III.

We see that the two techniques for obtaining σ_{3N} (coincidence phase space and singles) yield answers which just agree within the experimental uncertainties. One might suppose that we overestimated the values of f from the coincidence data. This could happen if the tail of the two-body process were contributing to the nonconjugate data. However, we examined the energy spectra of the nonconjugate coincidences and used only those spectra which exhibited no two-body peak [Figs. 4(a) and (b), for example]. Despite this precaution it appears that there is a peaking of the nonconjugate coincidence in the reaction plane defined by the incident pion and proton detected in the NaI telescope for a certain combination of angles. Vertical correlations at nonconjugate angles are shown in Figs. 12(a)–(c) (62.5 MeV π^+) and (d) (82.8 MeV/ π^+), together with the corresponding phase space calculations.

The two-body absorption cross section is simply determined from the A_0 coefficient. For $\pi^-+{}^3\mathrm{He}\rightarrow\mathrm{pn}+\mathrm{n}$, $\sigma_{2N}(\pi^-)=4\pi A_0$ and for $\pi^++{}^3\mathrm{He}\rightarrow\mathrm{pp}+\mathrm{p}$, $\sigma_{2N}(\pi^+)=2\pi A_0$ (integrate over 2π because of the indistinguishability of the coincident protons). The results are listed in Table IV. The errors do not include a total normalization uncertainty of 9% and 15% for the π^+ and π^- results, respectively.

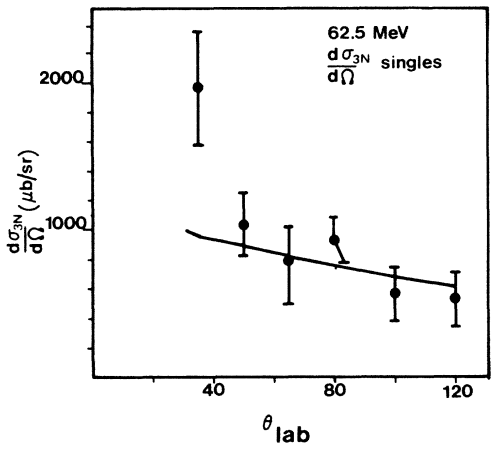

FIG. 11. Laboratory differential cross section for the three-body absorption reaction as defined in Eq. (6). The curve is the angular variation of the phase space normalized to the points between 50° and 120°.

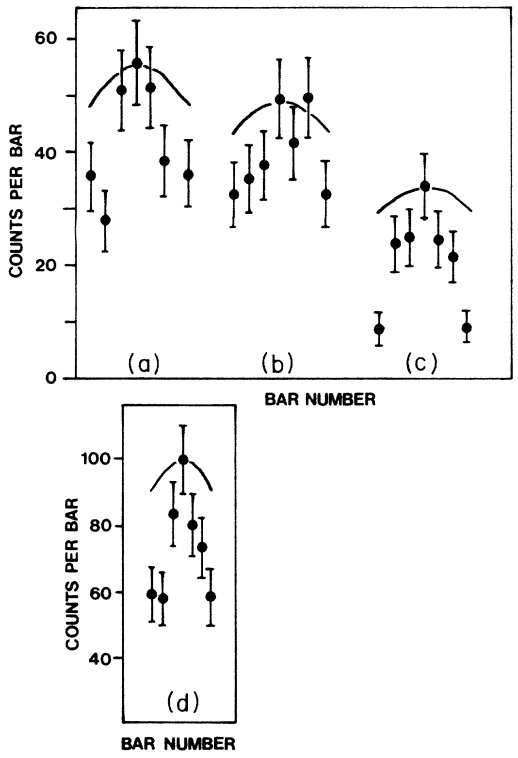

FIG. 12. Vertical angular correlation for nonconjugate or doubly nonconjugate coincidence for $\pi^+ + {}^3\text{He} \rightarrow \text{pp} + \text{p}$. The energy spectra showed no evidence for a two-body peak. Each point corresponds to the horizontal sum over an entire bar in the scintillator array. The angle pairs for the telescope and array are (θ_T, θ_A); (a) 62.5 MeV (65, −133); (b) 62.5 MeV (80, −114); (c) 62.5 MeV (40, −62); (d) 82.8 MeV (65, −129.9). The lines are the shapes expected from a phase space distribution normalized at the center of the angular correlation.

IV. DISCUSSION

A. Two-nucleon absorption process

From the values of σ_{2N} in Table IV and the $\pi + \text{d} \rightarrow \text{p} + \text{p}$ cross sections[9] we deduce the following values for the ratio $R_{QD} = \sigma(\pi^+ + {}^3\text{He} \rightarrow \text{pp} + \text{p}) / \sigma(\pi^+ + \text{d} \rightarrow \text{pp})$:

$$R_{QD}(62.5 \text{ MeV}) = 1.36 \pm 0.14 \tag{10a}$$

and

$$R_{QD}(82.8 \text{ MeV}) = 1.52 \pm 0.15, \tag{10b}$$

where the errors include the absolute uncertainties in both measurements. Moreover, the shapes of the angular distributions are indistinguishable from those of the $\pi^+ + \text{d} \rightarrow \text{p} + \text{p}$ reaction. For example, the ratios of the Legendre polynominal coefficients are

$$A_2/A_0 = 1.14 \pm 0.11 \text{ at } 62.5 \text{ MeV} \tag{11a}$$

and

$$A_2/A_0 = 1.10 \pm 0.07 \text{ at } 82.8 \text{ MeV} \tag{11b}$$

and should be compared to the average ratio[9] $\langle A_2/A_0 \rangle = 1.10 \pm 0.01$ for $\pi^+ + \text{d} \rightarrow \text{p} + \text{p}$ for $T_\pi = 65$–95 MeV.

The enhancement of the quasideuteron absorption in ^{3}He by a factor of about 1.5 is expected in the simplest model[3] which finds 1.5 p-n pairs in ^{3}He coupled to the deuteron quantum numbers. In view of the larger density of ^{3}He compared to the deuteron, it is surprising that an argument based only on Clebsch-Gordan coefficients gives the correct ratio. However, it was pointed out [18] that the shape of the short range correlation of the ^3S pair in ^{3}He and the deuteron were similar. For the large momentum transfer characteristic of pion absorption, this part of the wave function is the most important and this may explain the observed similarity.

Ohta, Thiess, and Lee[19] have calculated pion absorption cross sections at $T_\pi = 150$ MeV for absorption on the quasideuteron in ^{3}He compared to absorption on the deuteron. They find that absorption in ^{3}He is enhanced by 15% compared to the deuteron. The increase is small compared to the density difference between the deuteron and ^{3}He. They attribute this result to the long range nature of their two-body absorption operator.

The $\pi^+ + {}^3\text{He} \rightarrow \text{pp} + \text{p}$ angular correlation is interesting in that it, too, carries information about the reaction process. As noted in the previous section the full-width-at-half-maximum value of the proton-proton angular correlation is about 12°. We modeled the angular correlation by assuming that the π^+ was absorbed on a proton-neutron pair of total momentum k, whose angular distribution for pion absorption was the same as that for the deuteron. In this model the quasideuteron differential cross section is

$$\frac{d\sigma}{d\Omega}\text{QD} \equiv \frac{\int_0^\infty p(k) \frac{d\sigma_D}{d\Omega}(s) d^3k}{\int_0^\infty p(k) d^3k} . \tag{12}$$

Here s is the total center-of-mass energy for a particular choice of k; $p(k)$ is the probability for finding a nucleon pair with total momentum k.

The probability $p(k)$ was determined from the ^{3}He(e,e'p)d results of Ref. 20. We investigated the sensitivity of the angular correlation to the form of the 2N absorption cross section used in Eq. (12). An isotropic, energy-independent, differential cross section gave nearly identical results to that of the $\pi + \text{d} \rightarrow \text{p} + \text{p}$ differential cross section. Hence, the angular correlation is basically sensitive to the spectator nucleon momentum. The calculated and measured angular correlations are compared in Fig. 13.

The measured probability $p(k)$ from Ref. 20 reproduces the observed angular-correlation full-width-at-half-maximum of 12°. This result is in accord with the spectator model of the absorption process, in which the spectator nucleon emerges with the same momentum after the absorption that it had in the original ^{3}He nucleus. The width of the energy peak in the proton singles spectrum is also related to the internal momentum in ^{3}He. In an ear-

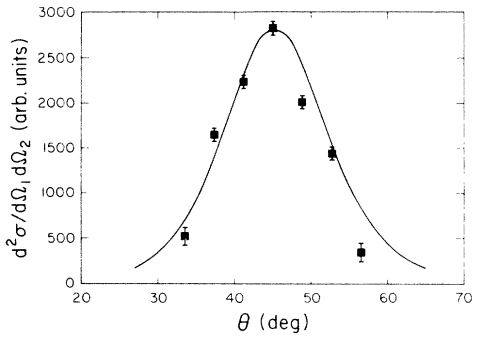

FIG. 13. Angular correlation taken at 165 MeV with one proton detected at 120°. The line is calculated by a spectator model with momentum distribution taken from (e,e'p) data.

lier measurement[21] of the singles spectrum from the $\pi^+ + {}^3\mathrm{He} \rightarrow \mathrm{pp} + \mathrm{p}$ reaction it was concluded that internal momenta greater than about 60 MeV/c were not significantly contributing to the absorption.

In the case of the π^- 2N absorption, the angular distributions at both energies (Figs. 8 and 9) are asymmetric about 90°. This may be due to interference between the 2N amplitude and 3N amplitude. On the other hand, the asymmetry may be a signature of a mixture of even and odd partial waves in the 2N amplitude. Previous discussions[3,5] have shown that at low pion bombarding energies, the $l_{\pi 2N}=0,1$ waves are the most likely contributions to the angular distribution. In the case of $l_{\pi 2N}=1,\pi^-$ absorption on the $T=1$, $S=0$ p-p pair proceeds through an intermediate state with isospin $=0$.

We made the assumption that at these energies only $l_\pi=0,1$ partial waves are contributing to the reaction. This assumption is marginally justified if we consider the kr values, using the deuteron radius. We note, however, that measurements of pion absorption on the deuteron at these energies do not detect any contribution from higher partial waves and that the present results do not show that higher order Legendre polynomials are needed to fit the angular distributions. With this assumption, we can calculate the coefficients of the Legendre polynomials by using the method of Blatt and Biedenharn.[22] The coefficients are given by

$$A_L = \sum Z(l_1 J_1 l_2 J_2, SL) Z(l_1' J_1' l_2' J_2', S'L) f , \tag{13}$$

where the unprimed quantum numbers are for the entrance channel and the primed ones are for the exit channel. Although these coefficients were originally defined to yield absolute values of cross sections, in the ensuing discussion we normalize the coefficients A_1 and A_2 to A_0, that is, to the cross section for the absorption process. The coefficients f contain the amplitudes and phases for each transition; they depend on the quantum numbers but not on L. The coefficients Z are calculated by angular momentum algebra,

$$Z(l_1 J_1 l_2 J_2, SL) = i^{L-l-1} 2(2l_1+1)^{1/2}(2l_2+1)^{1/2}(2J_2+1)^{1/2} W(l_1 J_1 l_2 J_2; SL)(l_1 l_2 00 \mid L\,0) . \tag{14}$$

We describe the transitions as follows: If δ is the amplitude for the reaction with $l_{\pi 2N}=0$ ($J^\pi=0^-$), then $(1-\delta^2)^{1/2}$ is for $l_{\pi 2N}=1$ ($J^\pi=1^+$) and there is a phase between the two. For the exit channel we denote by α the decay via $l'_{2N}=0$ and $(1-\alpha^2)^{1/2}$ is for decay via $l'_{2N}=2$, both allowed in the case of $J^\pi=1^+$, (Table I) and there is a phase between the two. Only one value, $L'_{2N}=1$, is allowed for the case $J^\pi=0^-$. We then compare the calculated coefficients with the measured and solve for the values of α^2 and δ^2. Since we have four unknowns and two equations, we obtain an area in the α^2 vs δ^2 plane with allowed solutions. The results are illustrated in Fig. 14.

The conclusion from these calculations is that at these bombarding energies the absorption on the proton pair is dominated by the $l_{\pi 2N}=1$ transition ($\sim$70% from Fig. 14). The errors in the measured coefficient do not alter this result qualitatively.

This transition has a total J^π value of 1^+, total isospin $T=0$, and therefore does not allow the formation of the delta resonance as an intermediate state. We note that if a delta resonance is formed (e.g., through $l_{\pi 2N}=0$), it cannot form together with the second nucleon a system with a relative angular momentum $L_{\Delta N}=0$, which is the dominant transition in pion absorption on the deuteron. It was noted by Silbar and Piasetzky[23] that a P_{11} isobar, if formed in the process of pion absorption on a ${}^1S_0$ $T=1$ nucleon pair, could form with the second nucleon a system with a relative angular momentum $L=0$. Their calculation of the angular distribution is shown by the dashed line in Fig. 8. The dominance of the $l_{\pi 2N}=1$ transition discussed above may indicate that the P_{11} isobar plays a role in this absorption process, similar to that played by the delta for pion absorption on the deuteron. The results of the calculations do not determine well the

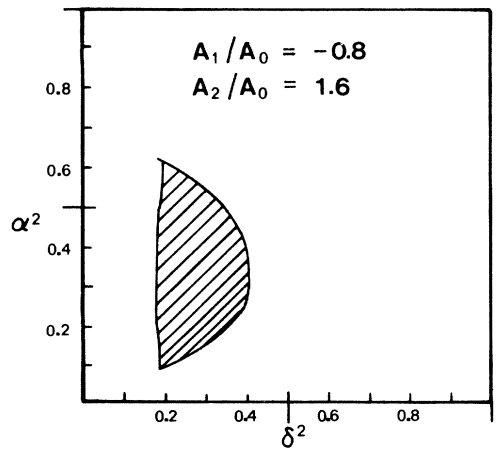

FIG. 14. Region of allowed solutions for α^2 and δ^2 for the $\pi^- + 2\mathrm{p} \rightarrow \mathrm{p} + \mathrm{n}$ reaction. δ is the normalized amplitude for pion absorption proceeding from the $l_{\pi 2N}=0$ initial channel and α is the normalized amplitude for $l'_{2N}=0$ in the exit channel.

relative amount of $l'_{2N}=0$ and $l'_{2N}=2$ transitions but tend to suggest a significant $l'_{2N}=2$ contribution (needed to generate the large anisotropy). This is reminiscent of the dominance of the $^1D_2$ final state in pion absorption on the deuteron; here this role may be played by a $^3D_1$ state.

These results are intimately related to studies of inelasticities in N-N interactions. The inelasticities are parametrized by $\sigma_{T_iT_f}$ where T_iT_f are the isospin values of the 2N systems in the incoming and outgoing channels, respectively. The much studied pp→dπ$^+$ reaction, for example, is characterized by $\sigma_{10}(d)$. The value of σ_{01} is the most difficult to study. It is obtained by combining the pn→ppπ$^-$ and pp→ppπ^0 reactions; the first measures $0.5(\sigma_{01}+\sigma_{11})$ and the second σ_{11}, and then subtracting. The subtraction procedure is very uncertain due to the mass difference between π$^-$ and π^0. The most recent results for the energy region of the present work[24] are upper limits of 200 μb. From the present results, we can deduce $\sigma_{01}(^1S_0)$, the analog of $\sigma_{10}(d)$. The cross sections listed in Table IV must be converted by detailed balance to the inverse reaction taking into account that in the present work the final 2N state is always a triplet. The results are 21.1 and 35.7 μb for 62.5 and 82.8 MeV, respectively. From Fig. 14 we can deduce that 0.7±0.2 of that is in the $T=0$ channel and we can therefore deduce $\sigma_{01}(^1S_0)$ values of 19±4 and 31±6 μb for 62.5 and 82.8 MeV (401 and 442 MeV for the inverse reaction), respectively. The great advantage of $\sigma_{01}(d)$ over σ_{10} is that it refers to well-defined quantum numbers in all states and as a consequence has been referred to in theoretical calculation much more than any other inelasticity. It is expected that the values of $\sigma_{01}(^1S_0)$, which also refer to well-defined quantum numbers, will have a similar impact.

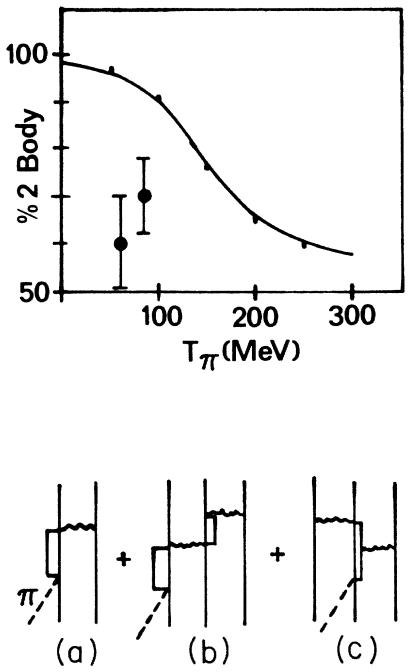

FIG. 15. Top—percentage of $\sigma_{2N}/(\sigma_{2N}+\sigma_{3N})$ for π$^+$ absorption on the p-n pair in ^{3}He (ϕ, this experiment) using nonconjugate angle data to determine σ_{3N}. The line is a calculation by Ref. 25. Bottom—processes considered by Ref. 25.

B. Three-body absorption

The total three-body cross sections at both energies and for both π$^+$ and π$^-$ are equal within experimental errors and are about half of the two-body ($T=0$, $J=1$) absorption cross sections. It is not likely that a large portion of the two-body absorption process was misidentified, because of final state interactions, as the three-body process. We saw in the previous discussion that the angular correlation for the (π$^+$,pp) reaction was only 12° wide FWHM, in agreement with spectator model calculations. Any interaction of the outgoing nucleon with the spectator nucleon would simply add to the width of the angular correlation. Hence, any proton-proton coincidences lost because of the scattering of an outgoing nucleon would have been compensated for in the correction for the array acceptance. Moreover, the simple prediction referred to earlier that $\sigma_{^3\mathrm{He}}(\pi^+ + \mathrm{pn}\rightarrow \mathrm{p}+\mathrm{p}) = 1.5\sigma(\pi^+ + \mathrm{d}\rightarrow \mathrm{p}+\mathrm{p})$ is verified.

Recently, calculations[25] of the relative importance of two- and three-nucleon absorption have been reported. In Fig. 15 we compare our results of the percentage $\sigma_{2N}/(\sigma_{2N}+\sigma_{3N})$ for π$^+$ absorption on the $T=0$ pair to these calculations. The agreement is not good. Experimentally the percentage of the two-body absorption is about 70% at our energies, whereas the predictions are that the two-body absorption is about 95% of the two-plus three-body absorption. This disagreement is surprising in light of the success these calculations have in fitting the energy dependence of pion absorption on ^{12}C and fitting the A dependence of the absorption cross section at T_π=165 MeV.

In the past, multinucleon modes of pion absorption have been deduced, sometimes indirectly, through a comparison of the cross section for quasideuteron absorption and the total absorption cross section.[7] Such a procedure relies on calculating the final state corrections and choosing the appropriate distortions for the pion and nucleon wave functions. In fact, it has recently been argued[26] that the background of the angular correlation[27] seen in ^{12}C(π$^+$,2p) at 165 MeV can be accounted for by a mixture of pion absorption on a quasideuteron in $L=0$ and $L=2$ states relative to the ^{10}B core. In the case of ^{3}He we have the advantage that the two-body angular correlation is narrow enough that off conjugate coincidences, relatively free from two-body coincidences, can be obtained. Hence we conclude that at our energies the three-body absorption is between 30% to 40% of the total true pion absorption on ^{3}He.

In conclusion, we present in this work measurements of two-body and three-body π absorption in ^{3}He at 62.5 and 82.8 MeV. For π$^+$, the two-body absorption cross sections have the same shape as for absorption on the deuteron with a magnitude which is about 50% larger. This indicates insensitivity of the absorption process to the ra-

dial wave function of the absorbing pair. For π^-, the two-body absorption cross sections have angular distributions which indicate that the process is dominated by $l_{\pi 2N}=1$ transitions which do not allow formation of the delta resonance as intermediate state. The P_{11} isobar may be playing an important role in this process. The three-body absorption, for both π^+ and π^-, appears to have a nearly constant matrix element, for a given bombarding energy, and thus the outgoing nucleons are distributed according to phase space. The magnitude of the three-body absorption is 42% and 60% of the two-body absorption at 82.8 and 62.5 MeV, respectively.

We wish to thank Dr. J. Schiffer for many valuable discussions. This work was supported in part by the Natural Sciences and Engineering Research Council of Canada and the Israel Commission for Basic Research. The work of U.W. was supported by the Deutscher Akademischer Austauschdienst.

*Present address: Department of Physics and Astronomy, California State University, Los Angeles, 5151 State University Drive, Los Angeles, CA 90032.

†Present address: Universität Basel, Klingelbergstrasse 82, 4056 Basel, Switzerland.

‡Present address: Swiss Institute for Nuclear Research, 5234 Villigen, Switzerland.

[1]K. Stricker, H. McManus, and J. A. Carr, Phys. Rev. C **19**, 929 (1979).

[2]D. Ashery, I. Navon, G. Azuelos, H. K. Walter, H. J. Pfeiffer, and F. W. Schlepütz, Phys. Rev. C **23**, 2173 (1981).

[3]D. Ashery, R. J. Holt, H. E. Jackson, J. P. Schiffer, J. R. Specht, K. E. Stephenson, R. D. McKeown, J. Ungar, R. E. Segel, and P. Zupranski, Phys. Rev. Lett. **47**, 895 (1981).

[4]P. Gotta, M. Dörr, W. Fetscher, G. Schmidt, H. Ullrich, G. Backenstoss, W. Howald, I. Schwanner, and H. J. Weyer, Phys. Lett. **112B**, 129 (1982).

[5]M. A. Moinester, D. R. Gill, J. Vincent, D. Ashery, S. Levenson, J. Alster, A. Altman, J. Lichtenstadt, E. Piasetzky, K. A. Aniol, R. R. Johnson, H. W. Roser, R. Tacik, W. Gyles, B. Barnett, R. J. Sobie, and H. P. Gubler, Phys. Rev. Lett. **52**, 1203 (1984).

[6]G. Backenstoss, M. Izycki, M. Steinacher, P. Weber, H. J. Weyer, K. von Weymarn, S. Cierjacks, S. Ljungfelt, U. Mankin, T. Petkovic, G. Schmidt, H. Ullrich, and M. Furic, Phys. Lett. **137B**, 329 (1984).

[7]D. Ashery, in Argonne National Laboratory Report ANL-PHY-83-1, CONF-830588, 1983.

[8]R. J. Kurz, University of California Report UCRL-1139, 1964 and 1965 (unpublished); H. Ullrich, D. Gotta, and T. Maiers, private communication.

[9]B. G. Ritchie, G. S. Blanpied, R. S. Moore, B. M. Preedom, K. Gotow, R. C. Minehart, J. Boswell, G. Das, H. J. Ziock, N. S. Chant, P. G. Roos, W. J. Burger, S. Gilad, and R. P. Redwine, Phys. Rev. C **27**, 1685 (1983).

[10]G. Fournier, A. Gérard, J. Miller, J. Picard, B. Saghai, P. Vernin, P. Y. Bertin, B. Coupat, E. W. A. Lingeman, and K. Seth, Nucl. Phys. **A426**, (1984) 542.

[11]G. J. Loos, E. L. Mathie, G. Jones, E. G. Auld, G. Giles, B. McParland, P. L. Walden, and W. Ziegler, Nucl. Phys. **A238**, 477 (1982).

[12]D. F. Measday and C. Richard-Serre, Nucl. Instrum. Methods **76**, 45 (1969).

[13]W. Dutty, J. Franz, E. Rössle, H. Schmitt, L. Schmitt, and O. Dumbrajs, in *Proceedings of the 10th International Conference on Few Body Problems in Physics, Karlsruhe, 1983,* edited by B. Zeitwitz (North-Holland, Amsterdam, 1984).

[14]J. Källne, J. E. Bolger, M. J. Devereaux, and S. L. Verbeck, Phys. Rev. C **24**, 1102 (1981).

[15]H. Fearing, Phys. Rev. C **16**, 313 (1977).

[16]B. H. Silverman, Ph.D. thesis, UCLA, 1982 (unpublished).

[17]R. Hagedorn, *Relativistic Kinematics* (Benjamin, New York, 1963).

[18]E. Hadjimichael, S. N. Yang, and G. E. Brown, Phys. Lett. **39B**, 594 (1972).

[19]K. Ohta, M. Thiess, and T.-S. H. Lee, Ann. Phys. (N.Y.) **163**, 420 (1985).

[20]E. Jans, P. Barreau, M. Bernheim, J. M. Finn, J. Morgenstern, J. Mougey, D. Ternowski, S. Turck-Chieze, S. Frullani, F. Garibaldi, G. P. Capitani, E. de Sanctis, M. K. Brussel, and I. Sick, Phys. Rev. Lett. **49**, 974 (1982).

[21]J. Källne, R. C. Minehart, R. R. Whitney, R. L. Boudrie, J. B. McClelland, and A. W. Stetz, Phys. Rev. C **28**, 304 (1983).

[22]J. M. Blatt and L. C. Biedenharn, Rev. Mod. Phys. **24**, 258 (1952).

[23]R. E. Silbar and E. Piasetzky, Phys. Rev. C **29**, 1116 (1984); **30**, 1365(E) (1984).

[24]M. Kleinschmidt, Th. Fischer, G. Hammel, W. Hürster, K. Kern, L. Lehman, E. Rössle, and H. Schmitt, Z. Phys. A **298**, 253 (1980).

[25]E. Oset, Y. Futami, and H. Toki, Proceedings of the International Conference on Particles and Nuclei, 1984, Heidelberg.

[26]B. G. Ritchie, N. S. Chant, and P. G. Roos, Phys. Rev. C **30**, 969 (1984).

[27]A. Altman, E. Piasetzky, J. Lichtenstadt, A. I. Yavin, D. Ashery, R. J. Powers, W. Bertl, L. Felawka, H. K. Walter, R. G. Winter, and J.v.d. Pluym, Phys. Rev. Lett. **50**, 1187 (1983).